

World Journal of *Gastroenterology*

World J Gastroenterol 2021 April 14; 27(14): 1362-1523



OPINION REVIEW

- 1362 How far along are we in revealing the connection between metformin and colorectal cancer?
Berkovic MC, Mikulic D, Bilic-Curcic I, Mrzljak A

REVIEW

- 1369 Intracellular interferon signalling pathways as potential regulators of covalently closed circular DNA in the treatment of chronic hepatitis B
Goh ZY, Ren EC, Ko HL

MINIREVIEWS

- 1392 Artificial intelligence-assisted endoscopic detection of esophageal neoplasia in early stage: The next step?
Liu Y
- 1406 COVID-19 and the gastrointestinal tract: source of infection or merely a target of the inflammatory process following SARS-CoV-2 infection?
Troisi J, Venutolo G, Pujolassos Tanyà M, Delli Carri M, Landolfi A, Fasano A

ORIGINAL ARTICLE**Basic Study**

- 1419 Lipotoxic hepatocyte-derived exosomal miR-1297 promotes hepatic stellate cell activation through the PTEN signaling pathway in metabolic-associated fatty liver disease
Luo X, Luo SZ, Xu ZX, Zhou C, Li ZH, Zhou XY, Xu MY
- 1435 Cyanidin 3-glucoside modulated cell cycle progression in liver precancerous lesion, *in vivo* study
Matboli M, Hasanin AH, Hussein R, El-Nakeep S, Habib EK, Ellackany R, Saleh LA

Retrospective Cohort Study

- 1451 Stapled transperineal repair for low- and mid-level rectovaginal fistulas: A 5-year experience and comparison with sutured repair
Zhou Q, Liu ZM, Chen HX, Ren DL, Lin HC
- 1465 Impact of preoperative antibiotics and other variables on integrated microbiome-host transcriptomic data generated from colorectal cancer resections
Malik SA, Zhu C, Li J, LaComb JF, Denoya PI, Kravets I, Miller JD, Yang J, Kramer M, McCombie WR, Robertson CE, Frank DN, Li E

Retrospective Study

- 1483 Apolipoprotein E variants correlate with the clinical presentation of paediatric inflammatory bowel disease: A cross-sectional study
Glapa-Nowak A, Szczepanik M, Iwańczak B, Kwiecień J, Szaflarska-Popławska AB, Grzybowska-Chlebowczyk U, Osiecki M, Dziekiewicz M, Stawarski A, Kierkuś J, Banasiewicz T, Banaszkiwicz A, Walkowiak J

Observational Study

- 1497** Exploration of nucleos(t)ide analogs cessation in chronic hepatitis B patients with hepatitis B e antigen loss
Xue Y, Zhang M, Li T, Liu F, Zhang LX, Fan XP, Yang BH, Wang L

META-ANALYSIS

- 1507** T-tube *vs* no T-tube for biliary tract reconstruction in adult orthotopic liver transplantation: An updated systematic review and meta-analysis
Zhao JZ, Qiao LL, Du ZQ, Zhang J, Wang MZ, Wang T, Liu WM, Zhang L, Dong J, Wu Z, Wu RQ

ABOUT COVER

Editorial Board Member of *World Journal of Gastroenterology*, Takuya Watanabe, MD, PhD, Director, Department of Internal Medicine and Gastroenterology, Watanabe Internal Medicine Aoyama Clinic, Aoyama 1-2-21, Nishi-ku, Niigata 950-2002, Japan, nabetaku@dia-net.ne.jp

AIMS AND SCOPE

The primary aim of *World Journal of Gastroenterology* (WJG, *World J Gastroenterol*) is to provide scholars and readers from various fields of gastroenterology and hepatology with a platform to publish high-quality basic and clinical research articles and communicate their research findings online. WJG mainly publishes articles reporting research results and findings obtained in the field of gastroenterology and hepatology and covering a wide range of topics including gastroenterology, hepatology, gastrointestinal endoscopy, gastrointestinal surgery, gastrointestinal oncology, and pediatric gastroenterology.

INDEXING/ABSTRACTING

The WJG is now indexed in Current Contents®/Clinical Medicine, Science Citation Index Expanded (also known as SciSearch®), Journal Citation Reports®, Index Medicus, MEDLINE, PubMed, PubMed Central, and Scopus. The 2020 edition of Journal Citation Report® cites the 2019 impact factor (IF) for WJG as 3.665; IF without journal self cites: 3.534; 5-year IF: 4.048; Ranking: 35 among 88 journals in gastroenterology and hepatology; and Quartile category: Q2. The WJG's CiteScore for 2019 is 7.1 and Scopus CiteScore rank 2019: Gastroenterology is 17/137.

RESPONSIBLE EDITORS FOR THIS ISSUE

Production Editor: Ji-Hong Liu, Production Department Director: Yun-Xiaojuan Wu, Editorial Office Director: Ze-Mao Gong.

NAME OF JOURNAL

World Journal of Gastroenterology

ISSN

ISSN 1007-9327 (print) ISSN 2219-2840 (online)

LAUNCH DATE

October 1, 1995

FREQUENCY

Weekly

EDITORS-IN-CHIEF

Andrzej S Tarnawski, Subrata Ghosh

EDITORIAL BOARD MEMBERS

<http://www.wjgnet.com/1007-9327/editorialboard.htm>

PUBLICATION DATE

April 14, 2021

COPYRIGHT

© 2021 Baishideng Publishing Group Inc

INSTRUCTIONS TO AUTHORS

<https://www.wjgnet.com/bpg/gerinfo/204>

GUIDELINES FOR ETHICS DOCUMENTS

<https://www.wjgnet.com/bpg/GerInfo/287>

GUIDELINES FOR NON-NATIVE SPEAKERS OF ENGLISH

<https://www.wjgnet.com/bpg/gerinfo/240>

PUBLICATION ETHICS

<https://www.wjgnet.com/bpg/GerInfo/288>

PUBLICATION MISCONDUCT

<https://www.wjgnet.com/bpg/gerinfo/208>

ARTICLE PROCESSING CHARGE

<https://www.wjgnet.com/bpg/gerinfo/242>

STEPS FOR SUBMITTING MANUSCRIPTS

<https://www.wjgnet.com/bpg/GerInfo/239>

ONLINE SUBMISSION

<https://www.f6publishing.com>

Basic Study

Cyanidin 3-glucoside modulated cell cycle progression in liver precancerous lesion, *in vivo* study

Marwa Matboli, Amany H Hasanin, Reham Hussein, Sarah El-Nakeep, Eman K Habib, Rawan Ellackany, Lobna A Saleh

ORCID number: Marwa Matboli 0000-0002-6852-3954; Amany H Hasanin 0000-0002-8018-4350; Reham Hussein 0000-0001-8591-3244; Sarah El-Nakeep 0000-0003-2830-5052; Eman K Habib 0000-0001-8899-6057; Rawan Ellackany 0000-0002-8591-3244; Lobna A Saleh 0000-0002-7987-8777.

Author contributions: Matboli M and Hasanin AH conceived the presented idea, developed the theory; Matboli M performed the statistics and the molecular assay; Hasanin AH verified the analytical methods; Hussein R and Saleh LA carried out the experimental animal work, performed the statistical analysis, writing the manuscript; El-Nakeep S developed the theory and writing the manuscript; Ellackany R has shared in the revision of the manuscript; Habib EK performed the histopathological examination and writing the comments; all authors discussed the results and contributed to the final manuscript revision.

Institutional animal care and use committee statement: All animal procedures were approved by the Institutional Animal Ethics Committee for Ain Shams University, Faculty of Medicine.

Marwa Matboli, Department of Biochemistry, Ain Shams Faculty of Medicine, Cairo 11318, Egypt

Amany H Hasanin, Reham Hussein, Lobna A Saleh, Department of Clinical Pharmacology, Ain Shams Faculty of Medicine, Cairo 11381, Egypt

Sarah El-Nakeep, Department of General Internal Medicine, Ain Shams Faculty of Medicine, Cairo 11381, Egypt

Eman K Habib, Department of Anatomy & Embryology, Ain Shams Faculty of Medicine, Cairo 11318, Egypt

Rawan Ellackany, Department of Undergraduate, Faculty of Medicine, Modern University for Technology and Information, Cairo 11381, Egypt

Corresponding author: Marwa Matboli, MD, Associate Professor, Department of Biochemistry, Ain Shams Faculty of Medicine, Abassia Marg, Cairo 11318, Egypt.
marwasayed472@yahoo.com

Abstract

BACKGROUND

Cyanidin-3-O-glucoside (cyan) exhibits antioxidant and anticancer properties. The cell cycle proteins and antimitotic drugs might be promising therapeutic targets in hepatocellular carcinoma.

AIM

To investigate the effect of cyan administration on cell cycle in hepatic precancerous lesion (PCL) induced by diethylnitrosamine/2-acetylaminofluorene (DEN/2-AAF) in Wistar rats.

METHODS

In vivo, DEN/2-AAF-induced hepatic PCL, rats were treated with three doses of cyan (10, 15, and 20 mg/kg/d, for four consecutive days *per week* for 16 wk). Blood and liver tissue samples were collected for measurement of the followings; alpha fetoprotein (AFP) liver function and RNA panel differential expression was evaluated *via* real time polymerase chain reaction. Histopathological examination of liver sections stained with H&E and immunohistochemical study using

Conflict-of-interest statement: No competing interest.

Data sharing statement: Data sharing not applicable to this article as no datasets were generated or analyzed during the current study.

ARRIVE guidelines statement: The authors have read the ARRIVE guidelines, and the manuscript was prepared and revised according to the ARRIVE guidelines.

Open-Access: This article is an open-access article that was selected by an in-house editor and fully peer-reviewed by external reviewers. It is distributed in accordance with the Creative Commons Attribution NonCommercial (CC BY-NC 4.0) license, which permits others to distribute, remix, adapt, build upon this work non-commercially, and license their derivative works on different terms, provided the original work is properly cited and the use is non-commercial. See: <http://creativecommons.org/licenses/by-nc/4.0/>

Manuscript source: Invited manuscript

Specialty type: Gastroenterology and hepatology

Country/Territory of origin: Egypt

Peer-review report's scientific quality classification

Grade A (Excellent): 0
Grade B (Very good): B, B
Grade C (Good): 0
Grade D (Fair): 0
Grade E (Poor): 0

Received: December 22, 2020

Peer-review started: December 22, 2020

First decision: January 17, 2021

Revised: January 22, 2021

Accepted: March 26, 2021

Article in press: March 26, 2021

Published online: April 14, 2021

P-Reviewer: Huang CY

S-Editor: Fan JR

L-Editor: A

glutathione S-transferase placental (GSTP) and proliferating cell nuclear antigen (PCNA) antibodies were assessed.

RESULTS

Cyan administration mitigated the effect of DEN/2-AFF induced PCL, decreased AFP levels, and improved liver function. Remarkably, treatment with cyan dose dependently decreased the long non-coding RNA MALAT1 and tubulin gamma 1 mRNA expressions and increased the levels of miR-125b, all of which are involved in cell cycle and mitotic spindle assembly. Of note, cyan decreased GSTP foci percent area and PCNA positively stained nuclei.

CONCLUSION

Our results indicated that cyan could be used as a potential therapeutic agent to inhibit liver carcinogenesis in rat model *via* modulation of cell cycle.

Key Words: Hepatocellular carcinoma therapy; Hepatocellular-carcinoma growth; Hepatocellular-carcinoma model; Hepatocellular-carcinoma size

©The Author(s) 2021. Published by Baishideng Publishing Group Inc. All rights reserved.

Core Tip: Several regulatory RNA networks are important in regulation of liver cell cycle progression and are linked to the pathogenesis of hepatocellular carcinoma. Identification of critical steps involved in hepatocarcinogenesis are likely to lead to the development of new therapeutics that will inhibit tumor proliferation alongside with verification of promising drug targets biomarkers that may lead to improved patient survival. Cyanidin-3-O-glucoside (cyan) has a significant antioxidant and anticancer activities. Cyan could be used as potential agent to inhibit liver carcinogenesis in rat model *via* modulation of cell cycle. Cyan dose dependently decreased the long non-coding RNA-MALAT1 and tubulin 1 mRNA expressions and increased the hsa-miR-125b expression which participate in cell cycle and mitotic spindle assembly.

Citation: Matboli M, Hasanin AH, Hussein R, El-Nakeep S, Habib EK, Ellackany R, Saleh LA. Cyanidin 3-glucoside modulated cell cycle progression in liver precancerous lesion, *in vivo* study. *World J Gastroenterol* 2021; 27(14): 1435-1450

URL: <https://www.wjgnet.com/1007-9327/full/v27/i14/1435.htm>

DOI: <https://dx.doi.org/10.3748/wjg.v27.i14.1435>

INTRODUCTION

Hepatocellular carcinoma (HCC) is the commonest primary malignancy of the liver. Its main risk factors include hepatitis B, hepatitis C, and non-alcoholic steatohepatitis. HCC is associated with high mortality and morbidity. Its incidence has increased from 1.4 to 6.2 *per* 100000 cases *per* year within the last 30 years^[1]. HCC burden in Egypt is high due to the high prevalence of HCV, where liver cancers account for 11.75% of all gastrointestinal cancers and 1.68% of all malignancies. In addition, over 70% of all liver malignancies in Egypt are HCC^[2].

To date, HCC is holding its place as an unresolved dilemma; its resistance to systemic chemotherapy and radiation makes the cure approachable only in very early stages according to Milan criteria, that is, where the tumor size is < 5 cm (when only one lesion is present) or < 3 cm (when 2-3 lesions are present)^[3].

Genes involved in cell cycle control are usually mutated in presence of cancer. Dysregulated mitosis results in genomic instability, which leads to tumor aggressiveness^[4]. Microtubules are a key component of mitotic spindles, and thus, a crucial part of the process of mitosis. They form an important target in cancer chemotherapy, inducing arrest of mitosis and cell death. On the other hand, while the overexpression of γ -tubulin (γ -TUBG) showed improved survival among small cell lung cancer patients^[5], the overexpression of γ -TUBG is found to be characteristic feature of thyroid and breast cancers^[6]. Such variation may arise due to differences in gene transcription and check point regulations in different cancer tissues^[7].

P-Editor: Wang LL



Cyanidin-3-glucoside (cyan) is a potential chemotherapeutic and chemo-protective agent. Through its antioxidant activity, it scavenges radical oxygen species, which decreases the overall number of tumorous cells (malignant and benign) in *in vivo* studies^[8]. Cyan has been implicated in some beneficial health activities^[9], including reducing age-associated oxidative stress^[10], improving cognitive brain function, and exhibiting anti-diabetic^[11], anti-inflammation^[12], anti-atherogenic^[13], and anti-obesity activities^[14]. Previously, it has been reported that cyan mediates caspase-3 cleavage with DNA fragmentation. Cyan has also been associated with induction of autophagy, a key element involved in cancer elimination, *via* induction of autophagy-related gene 5 and microtubule-associated protein 1 light chain 3-II^[15]. Cyan has drawn increasing attention because of its potential anti-cancer properties. Cyan may offer a novel avenue for treating HCC. a potential antiproliferative effect on HepG2 cells^[16].

The present study was conducted to evaluate the effect of cyan in three different doses on cell cycle progression and mitotic assembly disorder in hepatic precancerous lesion (PCL) *via* assessment of levels of long non-coding RNA (lncRNA) MALAT1, miR-125b, and tubulin 1. We also conducted histopathological and immunohistochemical examination using H&E staining assessment of levels of glutathione S-transferase placental (GSTP) and proliferating cell nuclear antigen (PCNA) antibodies in male Wistar rat model of diethylnitrosamine/2-acetyl-amino-fluorene (DEN/2-AAF)-induced hepatic PCL.

MATERIALS AND METHODS

Chemicals and drugs

DEN was obtained as 1 g solution in serum bottle diluted in 0.9% NaCl. 2-AAF was obtained as white powder, while cyan was obtained as black powder. Both 2-AAF and cyan were dissolved in 0.9% NaCl. All chemicals were purchased from Sigma-Aldrich, Cairo, Egypt.

Experimental animals

All animal procedures were approved by the Institutional Animal Ethics Committee of Ain Shams University, Faculty of Medicine. Thirty male Wistar rats weighing 200-250 g were purchased from Nile Pharmaceuticals Company (Cairo, Egypt). Animals were housed in an animal room with temperature 25 ± 2 °C and 12 h light/dark cycle controls. An adaptation period of 1 wk was allowed before initiation of the experimental protocol.

Experimental procedures

Induction of hepatic PCL: DEN was injected intraperitoneally (*i.p.*) at a dose of 100 mg/kg once weekly for three consecutive weeks. One week after the last DEN injection, a single dose (300 mg/kg) of 2-AAF was injected.

Animal groups: Rats were divided into five groups (6 rats/each group), including: Naïve group: Rats were injected with a vehicle (0.9% NaCl), PCL group: Rats were injected with DEN and 2-AAF, and three cyan groups (cyan-10, cyan-15, and cyan-20 groups): Rats were injected with DEN and 2-AAF, and orally administered through gastric gavage with cyan in doses of 10, 15, and 20 mg/kg respectively, for four consecutive days *per week* for 16 wk^[17].

Assessment of the effects of treatment

Biochemical and molecular studies: After scarifying the animals, blood was withdrawn from each rat from the retro orbital vein and incubated for about half an hour for clotting. Then, the blood sample was centrifuged for 20 min at 5000 RPM to get serum samples. Livers were dissected. The right lobe of the livers was removed, cut into longitudinal sections 2-4 mm in thickness and kept in 10% formalin for histopathological and immunohistochemical examination. The other lobe was kept frozen at -80 °C for molecular analyses. The samples were analyzed for the following parameters: (1) alpha fetoprotein (AFP) levels: AFP level was analyzed using quantitative sandwich rat AFP ELISA kit purchased from MyBiosource Inc. (San Diego, United States) with a sensitivity range of 0.625-20 ng/mL; (2) serum alanine aminotransferase (ALT) levels: The serum ALT was measured according to method described by using kits purchased from Diamond Diagnostic (Cairo, Egypt). ALT catalyzes the transfer of amino groups from specific amino acids to ketoglutaric acid, yielding glutamic acid and oxaloacetic or pyruvic acid, respectively. Ketoacids were

then determined calorimetrically after their reaction with 2, 4- dinitrophenylhydrazine; and (3) determination of serum total bilirubin and direct bilirubin: Alkaline methanolysis of bilirubin followed by chloroform extraction of bilirubin methyl esters, and later, separation of these esters by chromatography and spectrophotometric determination at 430 nm.

Determination of serum albumin

Quantitative determination of serum albumin level was quantified using rat albumin ELISA kit. The absorbance at 450 nm is a measure of the concentration of albumin in the test sample.

Bioinformatics-based selection of cell cycle-microtubule assembly- and HCC-specific RNA panel

The RNA panel was chosen in three steps: (1) *Tubulin, gamma 1 (TUBG1)* was retrieved as a crucial player in microtubule formation and progression of the cell cycle through gene atlas expression database (available at <https://www.ebi.ac.uk/gxa/home>) alongside with verification of the chosen gene from protein Atlas database (available at <https://www.proteinatlas.org/>), followed by analysis of *TUBG1* gene ontology to ensure that it is linked to G2-M transition and mitotic spindle assembly, which is closely linked to cancer development through gene card database (available at <https://www.genecards.org/>); (2) we selected miR-125b-1-3p targeting *TUBG1* mRNA through miRWalk database available at <http://mirwalk.umm.uni-heidelberg.de/>), followed by pathway enrichment, which revealed that miR-125b-1-3p is linked to MAP kinase and ubiquitin-mediated proteolysis (strongly correlated with mitotic assembly and cell cycle progression) through Diana database available at <http://diana.imis.athena-innovation.gr/DianaTools/index.php>); and (3) lncRNA metastasis-associated lung adenocarcinoma transcript 1, lncRNA MALAT1, was obtained as a lncRNA specific to HCC and targeting miR-125b-1-3p using noncode database available at <http://www.noncode.org/> and European Bioinformatics institute database available at <https://www.ebi.ac.uk>.

Extraction of total RNA, including lncRNA and miRNA from liver tissue

Total RNA was extracted from liver tissues using miRNeasy Mini kit (Cat No. 217004, Qiagen, United States) according to manufacturer's protocol. The extracted RNA concentration and integrity were assessed using [(NanoDrop Technologies/Thermo Scientific, Wilmington, DE, United States)], with RNA purities were 1.8-2. The extracted total RNA was reverse transcribed into cDNA using a miScript II RT kit (Cat No. 218160, 218161, Qiagen, United States) on thermal cycler (Bio-Rad; Hercules, CA, United States), according to the manufacturer's protocol.

Real time-polymerase chain reaction quantification of the RNA panel in liver tissues

The relative expression of *TUBG1* mRNA and lncRNA-MALAT1 in liver tissue were measured using a Quantitect SYBR Green Master Mix kit and an RT2 SYBR Green ROX real time-polymerase chain reaction (qPCR) Mastermix (Qiagen), respectively, using a 7500 qPCR Systems (Applied Biosystems, Foster City, CA, United States) detection system and specific primers (Accession: NM_001128148, NM_003234, NR_002819, and ENST00000534336, respectively) supplied by Qiagen. GAPDH (Accession NM_002046.7) was used as a housekeeping gene. MiR-3163 expression in liver tissue was quantified by PCR using a miScript SYBR Green kit (Qiagen), a miScript universal primer, and a miRNA-specific forward primer (mir-125b-1-3p miScript Primer Assay) (Accession: MIMAT0004592 (5'-ACGGGUUAGG CUCUUGGGAGCU). All steps followed the manufacturer's suggested protocol, and SNORD68 was used as an internal control. Ct values more than 36 were considered as negative. The specificities of the amplicons for the SYBR Green-based PCR amplification were affirmed by the melting curves. The $2^{-\Delta\Delta Ct}$ technique was used to measure the relative expression of the HCC-specific RNA panel.

Histopathological and immunohistochemical studies

Liver sections were cut at 5- μ m thickness and stained with H&E. Immunohistochemistry S-P method was used to detect GSTP and PCNA levels. Briefly, the protocol was as follows: (1) the tissues were treated with endogenous peroxidase blocking solution at room temperature for 10 min, and then, incubated in normal nonimmune serum at room temperature for 10 min; (2) mouse anti GSTP or PCNA antibody was added to adjacent tissue sections respectively and incubated overnight at 4 °C; (3) biotin-conjugated second antibody was added to the sections and incubated at

room temperature for 10 min; and (4) S-P complex was added at room temperature for 10 min, and then, 2,4-diaminobutyric acid was used for the color reaction. The tissue sections were washed with Poly (butylene succinate) (PBS) (0.01 mol/L, pH 7.4) between each step. Positive and negative controls were simultaneously used to ensure specificity and reliability of the staining process. A positive section was taken as positive control. In negative control, PBS was used to replace the first antibody. GSTP-positivity was indicated by brown coloration of the cytoplasm. Morphometric analysis of the foci percent area was carried out using Leica Q win V.3 software after capturing the images using a Leica DM2500 microscope (Leica, Wetzlar, Germany). The PCNA labeling indices are represented as the expression of positively-stained nuclei (10 fields/slide at 400 ×) as shown below: +, positive expression found in 1-3 fields; ++, positive expression found in 4-6 fields; and +++, positive expression found in 7-10 fields. Rabbit monoclonal PCNA and GSTP antibodies were purchased from Abcam (San Francisco, United States).

Statistical analysis

All results were expressed as mean ± SD. Statistical analysis was carried out using GraphPad Prism version 6.01. Unpaired t-test was done to compare between naïve and PCL groups. One-way ANOVA, followed by Tukey's test, was carried out to compare between all groups. *P* values < 0.05 were considered statistically significant.

RESULTS

Effect on AFP levels and liver function tests

As shown in **Figure 1**, following induction of PCL, rats exhibited a significant increase in AFP levels. AFP levels were significantly decreased in cyan-10, cyan-15, and cyan-20 groups compared to PCL group. There was no significant difference between the AFP levels of the three cyan groups. Liver function tests were affected after receiving DEN/2-AAF in which rats exhibited a significant increase in levels of ALT and total and direct bilirubin, and a significant decrease in the serum albumin (**Figure 2**). As shown in **Figure 2A**, rats received cyan. in different doses exhibited a significant decrease in serum ALT compared to PCL group. Cyan-15 group showed significant decrease in serum ALT compared to cyan-10 group. Moreover, cyan-20 group showed significant decrease in serum ALT compared to cyan-10 group. In As depicted in **Figure 2B**, compared to PCL group, the rats in the three cyan groups exhibited a significant decrease in serum total bilirubin. Furthermore, cyan-20 group showed significant decrease in serum total bilirubin compared to cyan-10 group. **Figure 2C**: Serum direct bilirubin was significantly decreased in the three cyan groups compared to the PCL group. Moreover, cyan-20 group showed significant decrease in serum direct bilirubin compared to cyan-10 group. Administration of cyan in doses 5, 10 and 20 mg/kg/d produced a significant increase in serum albumin compared to PCL group. However, there was no significant difference between the serum albumin levels of the three cyan groups (**Figure 2D**).

Effect on expression of lncRNA MALAT1, miR-125b, and TUBG1 (G2/M transition of mitotic cell cycle) in the liver tissue

As shown in **Figure 3**, induction of PCL resulted in significant increase of lncRNA MALAT1 a significant decrease in RQ miR-125b and significant increase in RQ TUBG1 expressions in comparison to naïve group. RQ of lncRNA MALAT1 in the liver tissue was significantly decreased in cyan -10,15 and cyan-20 groups compared to PCL group. Furthermore, cyan-20 group showed significant decrease in RQ of lncRNA MALAT1 in the liver tissue compared to cyan-10 group (**Figure 3A**). On the contrary, RQ of miR-125b in the liver tissue was significantly increased in cyan -10, cyan-15 and cyan-20 groups compared to PCL group. In addition, cyan-20 group showed significant increase in RQ of miR-125b in the liver tissue compared to cyan-10 group (**Figure 3B**). Furthermore, RQ of TUBG1 in the liver tissue was significantly decreased in cyan-10, cyan-15 and cyan-20 groups compared to PCL group. Also, cyan-20 group showed significant decrease in RQ of TUBG1 in the liver tissue compared to cyan-10 group (**Figure 3C**).

Histopathological and immunohistochemical studies

Light microscopic examination of H&E-stained sections of naïve rats' liver showed normal hepatic architecture, cords of hepatocytes radiating from central vein, portal

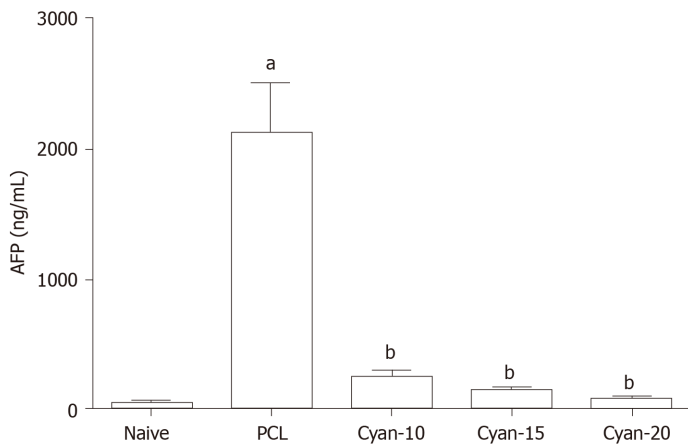


Figure 1 Effect of cyanidin 3-glucoside at different doses (10, 15 and 20 mg/kg/d) on alpha fetoprotein in the serum of rats. Values are mean \pm SEM; number of animals = 6 rats/each group. ^a $P < 0.05$ significant differences compared to naïve group, unpaired t test; ^b $P < 0.05$ significant differences compared to precancerous lesion group. PCL: Precancerous lesion; Cyan: Cyanidin-3-O-glucoside; AFP: Alpha fetoprotein.

triads present in between, polygonal hepatocytes with centrally rounded vesicular nuclei, and hepatic sinusoid in between (Figure 4A and B). Liver sections obtained from rats received DEN/2-AAF (Figure 4C-E) showed disruption of normal hepatic lobular architecture along with presence of large, discriminated dysplastic nodules compressing the surrounding liver tissue, with high-grade dysplastic cells displaying increased nuclear: Cytoplasmatic ratio (Figure 4E), nuclear hyperchromatosis, and basophilic cytoplasm. Liver sections of rats treated with different doses of cyanidin (10, 15, and 20 mg/kg) respectively, showed small and less discriminated dysplastic nodules (Figure 4F-H).

Immunohistochemical examination with GSTP antibody appeared as large hyperplastic nodules were demonstrated by the brown color. Figure 5A and B shows the liver sections of naïve group, while Figure 5C shows large-positively stained GSTP foci demonstrated in PCL group. Liver sections from rats of all cyan-treated groups exhibited small GSTP-positive small hepatic foci of different sizes scattered in-between negatively-stained hepatic parenchyma (Figure 5D-F). The percent area of GSTP foci was significantly increased in the PCL group compared to naïve group, while all cyan-treated groups showed significant decrease in the GSTP percent area. Furthermore, cyan-15 and -20 showed significant decrease in the GSTP percent area over cyan-10 (Table 1). PCNA immunohistochemical analysis showed an elevated expression of PCNA in the group that received DEN/2-AAF as compared to naïve group (Figure 6A and B). Liver sections obtained from rats received cyan. in its three doses showed decrease in PCNA-positively stained nuclei (Figure 6C-E and Table 1).

DISCUSSION

Altered expression of mitotic spindle assembly genes has been detected in many cancers. For example, *MAD2* gene levels are downregulated in breast carcinoma^[18], while mitotic checkpoint serine/*BUB1* gene expression is dysregulated in colorectal carcinoma^[19]. The impairment of spindle assembly genes are frequently detected in HCC^[20,21]. Moreover, inhibition of the mitotic assembly genes has been found to be lethal to cancer cells, and has promising therapeutic effect in cancer treatment^[22,23].

In this study, we used several public microarray databases for the construction of simple genetic-epigenetic network specific to HCC and linked to cell cycle and mitotic spindle formation. We assessed the antiproliferative effect of cyan in HCC animal model *via* modulation of lncRNA-MALAT1-miR-125b-TUBG1 mRNA axis expression.

Microtubules are involved both in maintenance of cell shape and motility and in mitotic spindle formation^[24]. γ -TUBG is a major player that supports microtubule nucleation. γ -TUBG acts as a binding site for the α/β -tubulin dimer and it has two γ -TUBG genes, TUBG1 and TUBG2 in mammals only^[25]. The TUBG levels in the centrosome change during cell cycle progression and usually increases at the start of mitosis. At the end of mitosis, TUBG levels are decreased to interphase levels^[26]. Overexpression and altered compartmentalization of γ -TUBG may lead to carcinogenesis^[27-29]. Interestingly, γ -TUBG associates interact with tumor suppressor

Table 1 Expression rate of hepatocytes positive for glutathione S-transferase placental and proliferating cell nuclear antigen were calculated as number of positive field expression in 10 fields *per rat* liver tissue

| | Naive | PCL | Cyan-10 | Cyan-15 | Cyan-20 |
|----------------------|-------------|--------------------------|--------------------------|----------------------------|----------------------------|
| GSTP +ve foci % area | 0.09 ± 0.07 | 47.2 ± 12.4 ^a | 33.4 ± 11.4 ^b | 8.95 ± 4.29 ^{b,c} | 3.83 ± 2.45 ^{b,c} |
| PCNA | | +++ | ++ | + | + |

Values are mean ± SD; number of animals = 6 rats/each group. Examined field; 10 fields/liver section.

^a*P* < 0.05 significant differences compared to naïve group.

^b*P* < 0.05 significant differences compared to precancerous lesion group.

^c*P* < 0.05 significant compared to cyanidin-3-O-glucoside-10, One-way ANOVA followed by Tukey's test. +: Positive expression found in 1-3 fields; ++: Positive expression found in 4-6 fields; +++: Positive expression found in 7-10 field; PCL: Precancerous lesion; Cyan: Cyanidin-3-O-glucoside; GSTP: Glutathione S-transferase placental; PCNA: Proliferating cell nuclear antigen.

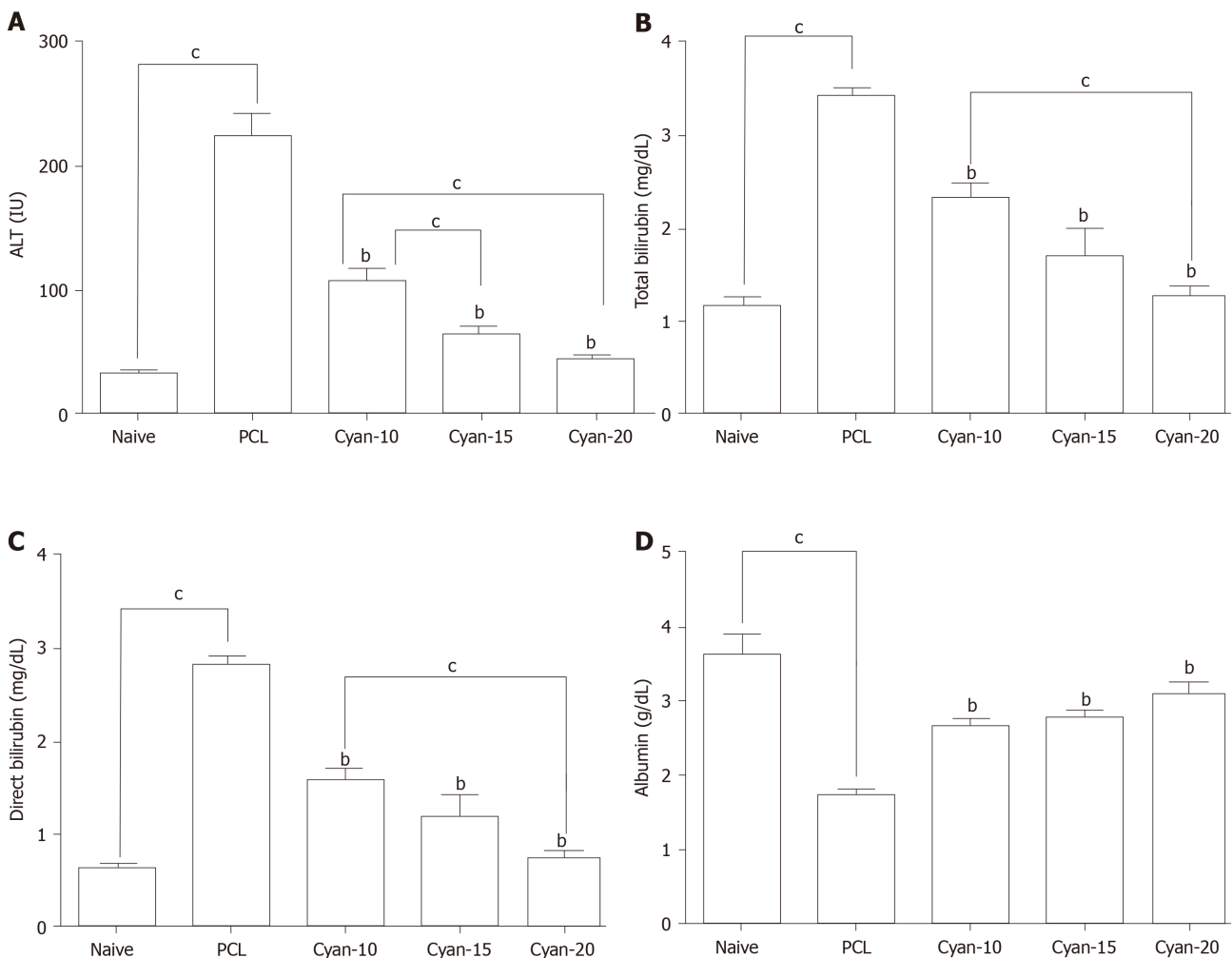


Figure 2 Effect of cyanidin 3-glucoside at different doses (10, 15 and 20 mg/kg/d) in rats. A: Alanine aminotransferase; B: Total bilirubin; C: Direct bilirubin; D: Serum albumin. Values are mean ± SEM; number of animals = 6 rats/each group. ^b*P* < 0.05 significant differences compared to precancerous lesion group; ^c*P* < 0.05 significant differences between the 2 selected groups, One-way ANOVA followed by Tukey's test. PCL: Precancerous lesion; Cyan: Cyanidin-3-O-glucoside; ALT: Alanine aminotransferase.

protein C53 in mammalian interphase cells of different cellular origins^[30]. Interestingly, γ -TUBG interacts with E2F transcription factors, resulting in upregulation of E2F target genes PCNA and CDKB1^[31] and glutathione S transferase activity^[32]. On the other hand, the mRNA and protein levels of TUBA1C are upregulated in HCC. Clinically, it affects the survival of patients and the level of metastatic burden along with portal vein thrombosis. In addition, it activates cellular proliferation and migration and is a potential therapeutic target for HCC^[33]. Recent studies have shed light on the efficacy of microtubule-binding agents in the treatment of HCC, especially

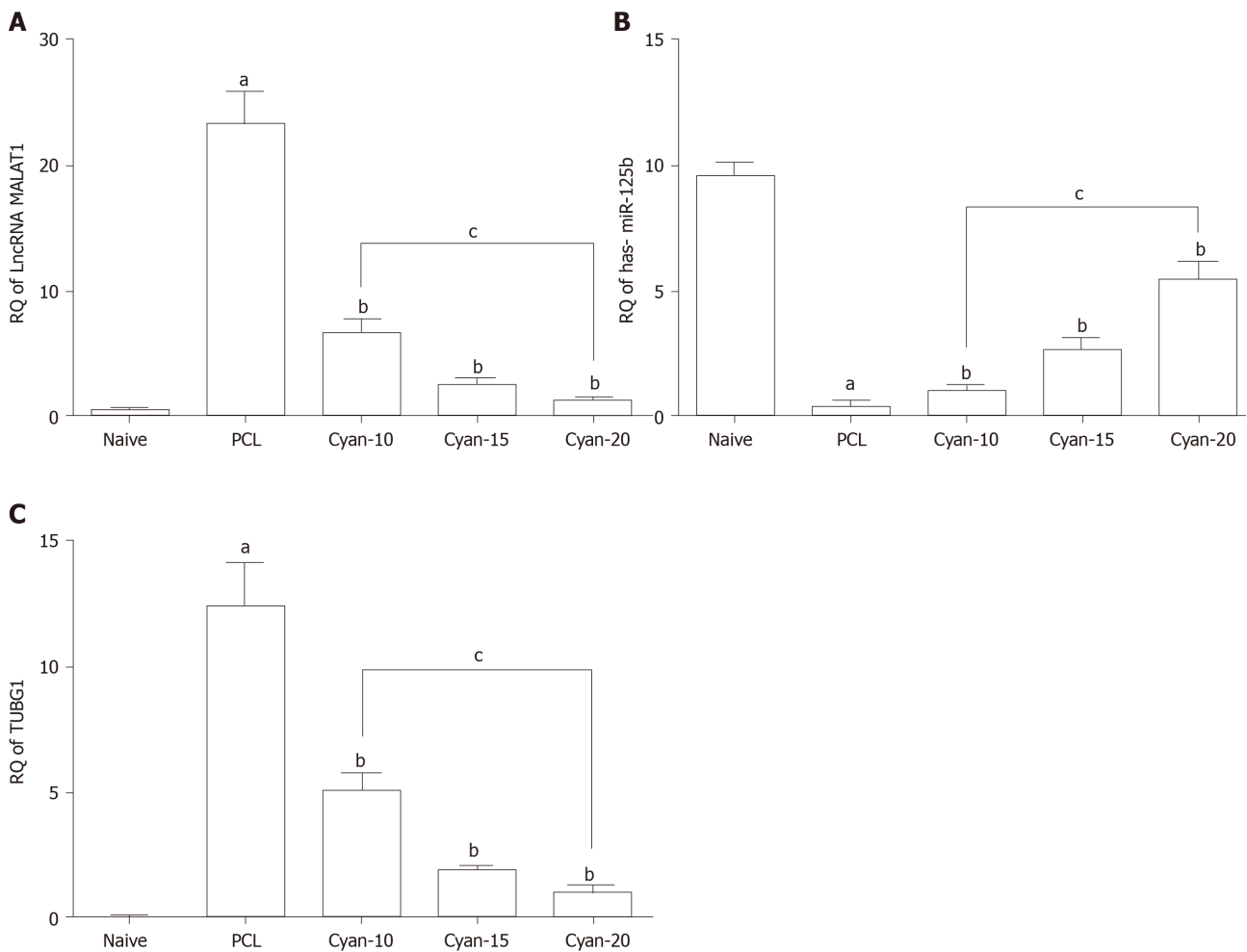


Figure 3 Effect on expression of long non-coding RNA, MALAT1, miR-125b and tubulin 1 (G2/M transition of mitotic cell cycle) in the liver tissue. A: RQ of long non-coding RNA MALAT1; B: RQ miR-125b; C: RQ TUBG1. Values are mean \pm SEM; number of animals = 6 rats/each group. ^a $P < 0.05$ significant differences compared to naive group; ^b $P < 0.05$ significant differences compared to precancerous lesion group; ^c $P < 0.05$ significant differences between the 2 selected groups, One-way ANOVA followed by Tukey's test. PCL: Precancerous lesion; Cyan: Cyanidin-3-O-glucoside; TUBG: Tubulin gamma 1; lncRNA: Long non-coding RNA.

in combination with mammalian target of rapamycin inhibitors^[34].

One of the few miRNAs that regulate Spindle Assembly Checkpoints (SAC) is miR-125b. It suppresses the expression of Mad1 (a core SAC protein) that is responsible for inhibiting entry into anaphase till metaphase defects are corrected^[35]. Importantly, miRNA-125b has been found to be associated with colorectal cancer^[36], multiple myeloma^[37], and breast cancer^[38]. Song *et al*^[39] demonstrated that the expression of miR-125b in hepatocytes was protective and reflected better survival in HCC tissue samples due to restoration of SIRT6 expression^[39]. miR-125b-5p inhibits HCC proliferation by targeting TXNRD1, the terminal step of biosynthesis of nucleotides^[40].

Deregulation of lncRNAs has been shown to be crucial in cancer progression, especially HCC^[41,42]. Hung *et al*^[43] demonstrated the involvement of lncRNAs in regulation of the expression of cell cycle-related genes, p53 gene regulatory pathway, and apoptosis^[43,44]. The lncRNA MALAT1 is overexpressed in several solid tumors and is linked with tumor recurrence^[45-47]. MALAT1 coordinate RNA polymerase II transcription, pre-mRNA splicing, and mRNA export^[48]. Thus, this lncRNA holds great potential in influencing the local concentration of a specific splicing factor during specific stages of the cell cycle. Depletion of MALAT1 in cancer cells inhibits tumorigenicity^[49]. MALAT1 regulates E2F1 transcription factor activity, highlighting its pro-proliferative function^[50]. MALAT1 is upregulated in many cancer types, including breast cancer^[51], cervical cancer, lung cancer^[52], and hepatocarcinoma^[53-55]. In a previous study, hypoxia enhanced MALAT1 expression, leading to increase in proliferating and invading activity of Hep3B cells due to negative interaction with miR200a^[56]. Huang and his group explored the role of specificity protein 1/3 in regulation of MALAT1 expression in HCC cells^[57].

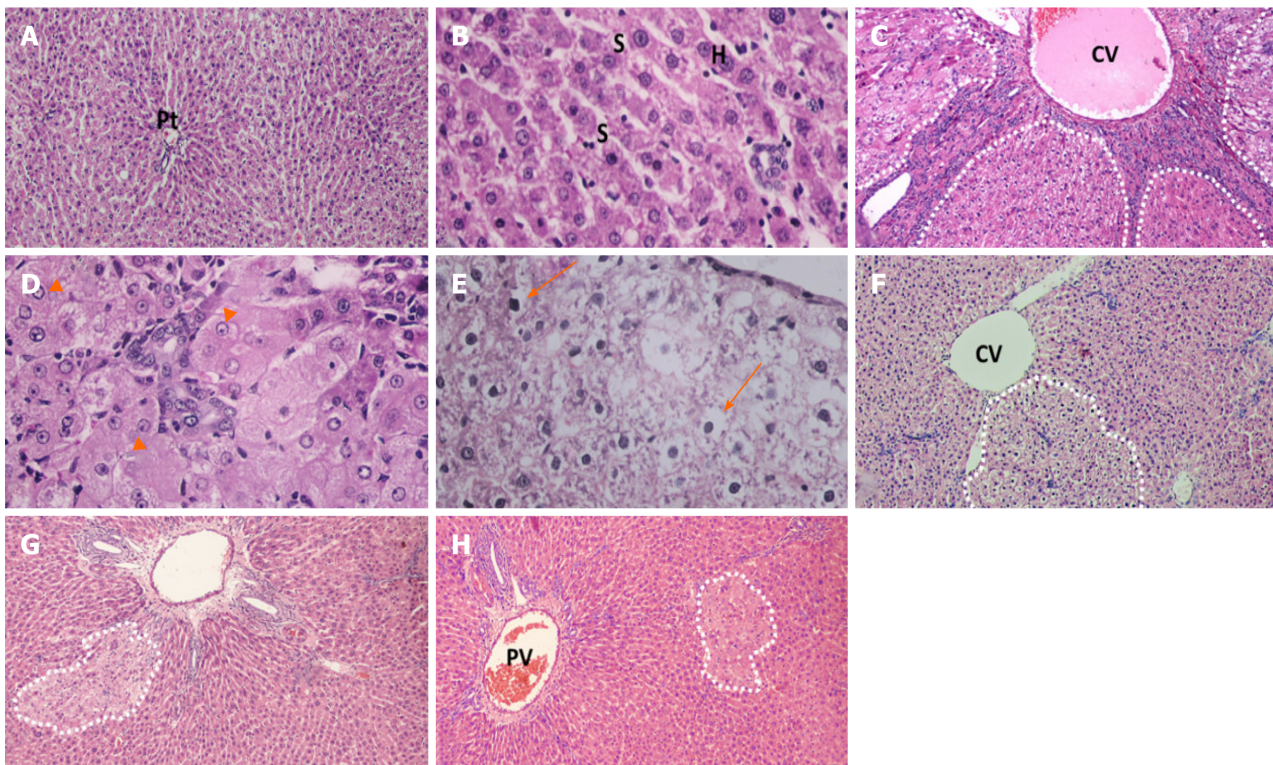


Figure 4 Photomicrographs of liver sections stained with H&E staining. A and B: Naïve group liver sections showed normal hepatic architecture, cords of hepatocytes radiating from central vein and portal triads present in-between and polygonal hepatocytes with central rounded vesicular nuclei, and hepatic sinusoid in-between; C-E: Liver sections of rats received diethylnitrosamine/2-acetylaminofluorene (DEN/2-AAF) showed larger, discriminated dysplastic nodules (dotted shapes) compressing the surrounding liver tissue with disruption of normal hepatic lobular architecture; D: Liver sections of rats received DEN/2-AAF showed eosinophilic foci of cellular alteration consisting of enlarged hepatocytes with increased acidophilic staining and vacuolated nuclei (arrow head); E: Liver sections of rats received DEN/2-AAF showed foci of Clear cell formed of hepatocytes showing variable degrees of cytoplasmic vacuolations and ballooning with pyknotic nuclei (arrow); F-H: Liver sections of rats treated with different doses of cyanidin (10, 15, 20 mg/kg) respectively, showing small and less discriminated dysplastic nodules (dotted shapes). (Magnification: A, C, F, G, H \times 1000; B, D, E \times 400). CV: Central vein; PV: Portal vein; Pt: Portal triads; S: Sinusoid; H: Hepatocytes.

Cyanidin or anthocyanin (a polyphenolic pigment found in plants) confers several pharmacological benefits, including anticancer properties^[58-62]. Cyan mediates cytotoxicity against human monocytic leukemia cells *via* G2/M phase arrest and induction of apoptosis^[63]. Tsai *et al.*^[64] evaluated anthocyanins as promising anticancer or chemopreventive agents to induce G2/M arrest in HAs-induced leukemia cell cycle arrest *via* ATM-Chk1/2-Cdc25C axis modulation^[64]. They also found that anthocyanin inhibits the proliferation of HCC cells^[65,66].

In our study, the effect of cyan on cancerous tissue was dose-dependent (10, 15 and 20 mg/kg/d), that is, increasing its effect with increasing the concentration of the drug. This was proved also, with the correlated significant decrease in the percent area of GSTP foci, PCNA expression which are the target of TUBG1 mRNA and the molecular epigenetic markers associated with HCC (lncRNA MALAT1 and miR-125b-1-3p) in the liver tissue of rats in our study (Figure 7). Thus, we can hypothesize that administration of cyan in PCL may result in downregulation of lncRNA MALAT1 with subsequent release of free miR-125b-1-3p that binds to TUBG1 mRNA and downregulate its expression^[65]. The changes in the epigenetic-genetic network affect their target genes PCNA and GSTP.

Lastly, the cyan-mediated modulation of cell cycle and mitotic spindle assembly that regulate HCC proliferation might affect the capability of the HCC cells to overcome oxidative stress^[66,67]. Our data confers the rationale for designing antimetabolic approach combining the conventional cytotoxic drugs with phytochemical extracts to inhibit cell cycle progression in cancer. More *in vitro* functional studies are required to explore the functional mechanism of the chosen RNA panel and validate their role as drug target biomarkers.

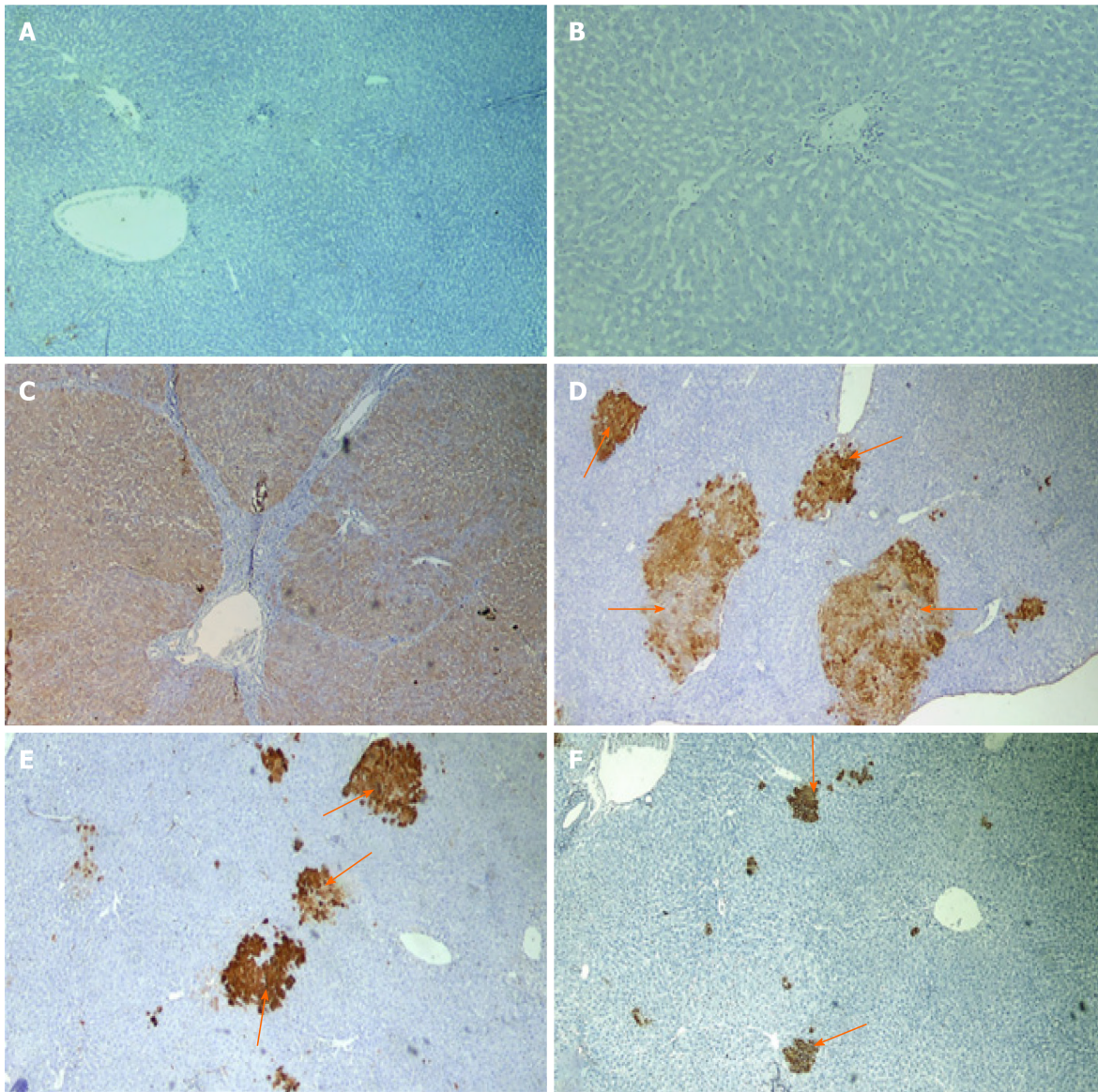


Figure 5 Photomicrographs of liver sections of rats immunohistochemical stained with glutathione S-transferase placental antibody. A and B: Naive group; C: Precancerous lesion group showing multiple glutathione S-transferase placental (GSTP)-positive large hepatic nodules (brown stained nodules) occupying most of section; D-F: Liver sections of rats treated with different doses of cyanidin (10, 15, 20 mg/kg) showing GSTP positive small hepatic foci (brown stained cells = arrow) of different size scattered in-between negatively stained hepatic parenchyma. (Magnification: $\times 40$)

CONCLUSION

Cyanidin is a natural molecule that holds great potential in unraveling the mystery of cytotoxic pharmacy in the future. It can be used to devise novel antimitotic drugs that can target cell cycle in HCC. Our results also indicated great potential of the TUBG1 mRNA- miR-125b-lncRNA MALAT1 and -1-3p axis as potential drug target biomarker for further investigations.

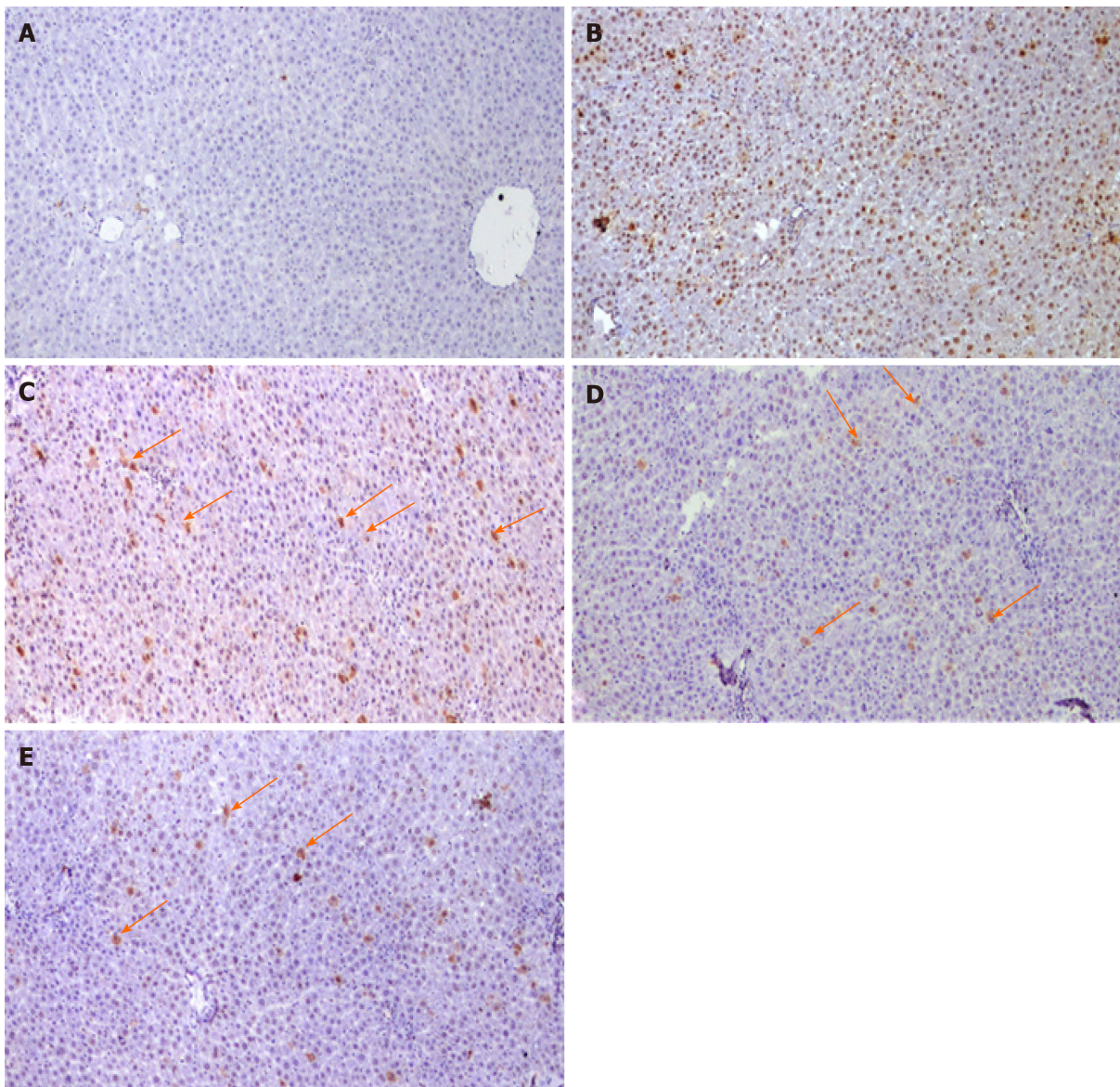


Figure 6 Photomicrographs of liver sections immunohistochemically stained with proliferating cell nuclear antigen. A: Negative reaction of control group; B: Diethylnitrosamine + 100 mg 2-acetylaminofluorene group showing positive stained nuclei scattered all over the field; C-E: Liver sections of rats treated with different doses of cyanidine (10, 15, 20 mg/kg) respectively, show few positive hepatocytes sporadically distributed over the field (arrow). (Magnification $\times 100$).

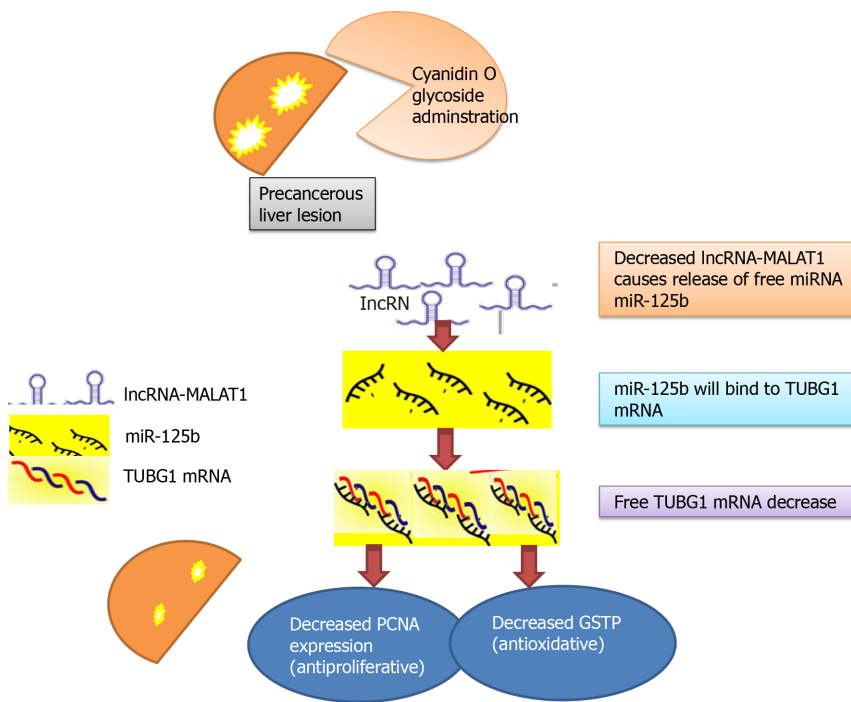


Figure 7 Concept map of study design. GSTP: Glutathione S-transferase placental; PCNA: Proliferating cell nuclear antigen; TUBG: Tubulin; IncRNA: Long non-coding RNA.

ARTICLE HIGHLIGHTS

Research background

Several regulatory RNA networks are important in regulation of liver cell cycle progression.

Research motivation

Cyanidin-3-glucoside (cyan) is a potential chemotherapeutic and chemo-protective agent.

Research objectives

The present study aimed to investigate the effect of cyan administration on cell cycle in hepatic precancerous lesion induced by diethylnitrosamine/2-acetylaminofluorene in Wistar rats.

Research methods

We used bioinformatic analysis followed by experimental validation.

Research results

Cyan dose dependently decreased the long non-coding RNA-MALAT1 and tubulin gamma 1 mRNA expressions and increased the hsa-miR-125b expression which participate in cell cycle and mitotic spindle assembly. Cyan administration decreased alpha-fetoprotein and improved liver function. Cyan decreased glutathione S-transferase placental foci percent area and proliferating cell nuclear antigen positively stained nuclei.

Research conclusions

Cyanidin may offer a natural molecule to unravel the mystery a cytotoxic pharmacy for the future.

Research perspectives

Further larger *in vitro* and *in vivo* studies are needed to elucidate the mechanism of cyanidin cytotoxicity in hepatocellular carcinoma.

REFERENCES

- 1 **Ghouri YA**, Mian I, Rowe JH. Review of hepatocellular carcinoma: Epidemiology, etiology, and carcinogenesis. *J Carcinog* 2017; **16**: 1 [PMID: 28694740 DOI: 10.4103/jcar.JCar_9_16]
- 2 **Holah NS**, El-Azab DS, Aiad HA, Sweed D. Hepatocellular carcinoma in Egypt: epidemiological and histopathological properties. *MMJ* 2015; **28**: 718-724 [DOI: 10.4103/1110-2098.173700]
- 3 **Kulik L**, El-Serag HB. Epidemiology and Management of Hepatocellular Carcinoma. *Gastroenterology* 2019; **156**: 477-491. e1 [PMID: 30367835 DOI: 10.1053/j.gastro.2018.08.065]
- 4 **Paier CRK**, Maranhão SS, Carneiro TR, Lima LM, Rocha DD, Santos RDS, Farias KM, Moraes-Filho MO, Pessoa C. Natural products as new antimetabolic compounds for anticancer drug development. *Clinics (Sao Paulo)* 2018; **73**: e813s [PMID: 30540125 DOI: 10.6061/clinics/2018/e813s]
- 5 **Maounis NF**, Dráberová E, Trakas N, Chorti M, Riga D, Tzannis K, Kanakis M, Voralu K, Ellina E, Mahera E, Demonakou M, Lioulis A, Dráber P, Katsetos CD. Expression of γ -tubulin in non-small cell lung cancer and effect on patient survival. *Histol Histopathol* 2019; **34**: 81-90 [PMID: 30010174 DOI: 10.14670/HH-18-027]
- 6 **Hořejší B**, Vinopal S, Sládková V, Dráberová E, Sulimenko V, Sulimenko T, Vosecká V, Philimonenko A, Hozák P, Katsetos CD, Dráber P. Nuclear γ -tubulin associates with nucleoli and interacts with tumor suppressor protein C53. *J Cell Physiol* 2012; **227**: 367-382 [PMID: 21465471 DOI: 10.1002/jcp.22772]
- 7 **Alvarado-Kristensson M**. γ -tubulin as a signal-transducing molecule and meshwork with therapeutic potential. *Signal Transduct Target Ther* 2018; **3**: 24 [PMID: 30221013 DOI: 10.1038/s41392-018-0021-x]
- 8 **Ding M**, Feng R, Wang SY, Bowman L, Lu Y, Qian Y, Castranova V, Jiang BH, Shi X. Cyanidin-3-glucoside, a natural product derived from blackberry, exhibits chemopreventive and chemotherapeutic activity. *J Biol Chem* 2006; **281**: 17359-17368 [PMID: 16618699 DOI: 10.1074/jbc.M600861200]
- 9 **Flores G**, Dastmalchi K, Paulino S, Whalen K, Dabo AJ, Reynertson KA, Foronjy RF, D'Armiento JM, Kennelly EJ. Anthocyanins from *Eugenia brasiliensis* edible fruits as potential therapeutics for COPD treatment. *Food Chem* 2012; **134**: 1256-1262 [PMID: 25005941 DOI: 10.1016/j.foodchem.2012.01.086]
- 10 **Nam DC**, Hah YS, Nam JB, Kim RJ, Park HB. Cytoprotective Mechanism of Cyanidin and Delphinidin against Oxidative Stress-Induced Tenofibroblast Death. *Biomol Ther (Seoul)* 2016; **24**: 426-432 [PMID: 27098861 DOI: 10.4062/biomolther.2015.169]
- 11 **Belwal T**, Nabavi SF, Nabavi SM, Habtemariam S. Dietary Anthocyanins and Insulin Resistance: When Food Becomes a Medicine. *Nutrients* 2017; **9** [PMID: 29023424 DOI: 10.3390/nu9101111]
- 12 **He Y**, Hu Y, Jiang X, Chen T, Ma Y, Wu S, Sun J, Jiao R, Li X, Deng L, Bai W. Cyanidin-3-O-glucoside inhibits the UVB-induced ROS/COX-2 pathway in HaCaT cells. *J Photochem Photobiol B* 2017; **177**: 24-31 [PMID: 29031211 DOI: 10.1016/j.jphotobiol.2017.10.006]
- 13 **Oak MH**, Bedoui JE, Madeira SV, Chalupsky K, Schini-Kerth VB. Delphinidin and cyanidin inhibit PDGF(AB)-induced VEGF release in vascular smooth muscle cells by preventing activation of p38 MAPK and JNK. *Br J Pharmacol* 2006; **149**: 283-290 [PMID: 16921400 DOI: 10.1038/sj.bjp.0706843]
- 14 **Du C**, Shi Y, Ren Y, Wu H, Yao F, Wei J, Wu M, Hou Y, Duan H. Anthocyanins inhibit high-glucose-induced cholesterol accumulation and inflammation by activating LXR α pathway in HK-2 cells. *Drug Des Devel Ther* 2015; **9**: 5099-5113 [PMID: 26379423 DOI: 10.2147/DDDT.S90201]
- 15 **Wu S**, Hu Y, Bai W, Zhao J, Huang C, Wen C, Deng L, Lu D. Cyanidin-3-o-glucoside inhibits UVA-induced human dermal fibroblast injury by upregulating autophagy. *Photodermatol Photoimmunol Photomed* 2019; **35**: 360-368 [PMID: 31166622 DOI: 10.1111/phpp.12493]
- 16 **Pace E**, Jiang Y, Clemens A, Crossman T, Rupasinghe HPV. Impact of Thermal Degradation of Cyanidin-3-O-Glucoside of Haskap Berry on Cytotoxicity of Hepatocellular Carcinoma HepG2 and Breast Cancer MDA-MB-231 Cells. *Antioxidants (Basel)* 2018; **7** [PMID: 29382057 DOI: 10.3390/antiox7020024]
- 17 **Qin L**, Zhang J, Qin M. Protective effect of cyanidin 3-O-glucoside on beta-amyloid peptide-induced cognitive impairment in rats. *Neurosci Lett* 2013; **534**: 285-288 [PMID: 23274703 DOI: 10.1016/j.neulet.2012.12.023]
- 18 **Li Y**, Benezra R. Identification of a human mitotic checkpoint gene: hsMAD2. *Science* 1996; **274**: 246-248 [PMID: 8824189 DOI: 10.1126/science.274.5285.246]
- 19 **Cahill DP**, Lengauer C, Yu J, Riggins GJ, Willson JK, Markowitz SD, Kinzler KW, Vogelstein B. Mutations of mitotic checkpoint genes in human cancers. *Nature* 1998; **392**: 300-303 [PMID: 9521327 DOI: 10.1038/32688]
- 20 **Liang XD**, Dai YC, Li ZY, Gan MF, Zhang SR, Yin-Pan, Lu HS, Cao XQ, Zheng BJ, Bao LF, Wang DD, Zhang LM, Ma SL. Expression and function analysis of mitotic checkpoint genes identifies TTK as a potential therapeutic target for human hepatocellular carcinoma. *PLoS One* 2014; **9**: e97739 [PMID: 24905462 DOI: 10.1371/journal.pone.0097739]
- 21 **Saeki A**, Tamura S, Ito N, Kiso S, Matsuda Y, Yabuuchi I, Kawata S, Matsuzawa Y. Frequent impairment of the spindle assembly checkpoint in hepatocellular carcinoma. *Cancer* 2002; **94**: 2047-2054 [PMID: 11932908 DOI: 10.1002/ncr.10448]
- 22 **Kops GJ**, Foltz DR, Cleveland DW. Lethality to human cancer cells through massive chromosome loss by inhibition of the mitotic checkpoint. *Proc Natl Acad Sci USA* 2004; **101**: 8699-8704 [PMID:

- 15159543 DOI: [10.1073/pnas.0401142101](https://doi.org/10.1073/pnas.0401142101)]
- 23 **Kops GJ**, Weaver BA, Cleveland DW. On the road to cancer: aneuploidy and the mitotic checkpoint. *Nat Rev Cancer* 2005; **5**: 773-785 [PMID: [16195750](https://pubmed.ncbi.nlm.nih.gov/16195750/) DOI: [10.1038/nrc1714](https://doi.org/10.1038/nrc1714)]
 - 24 **Ohashi T**, Yamamoto T, Yamanashi Y, Ohsugi M. Human TUBG2 gene is expressed as two splice variant mRNA and involved in cell growth. *FEBS Lett* 2016; **590**: 1053-1063 [PMID: [27015882](https://pubmed.ncbi.nlm.nih.gov/27015882/) DOI: [10.1002/1873-3468.12163](https://doi.org/10.1002/1873-3468.12163)]
 - 25 **Wise DO**, Krahe R, Oakley BR. The gamma-tubulin gene family in humans. *Genomics* 2000; **67**: 164-170 [PMID: [10903841](https://pubmed.ncbi.nlm.nih.gov/10903841/) DOI: [10.1006/geno.2000.6247](https://doi.org/10.1006/geno.2000.6247)]
 - 26 **Fant X**, Gnadt N, Haren L, Merdes A. Stability of the small gamma-tubulin complex requires HCA66, a protein of the centrosome and the nucleolus. *J Cell Sci* 2009; **122**: 1134-1144 [PMID: [19299467](https://pubmed.ncbi.nlm.nih.gov/19299467/) DOI: [10.1242/jcs.035238](https://doi.org/10.1242/jcs.035238)]
 - 27 **Maounis NF**, Dráberová E, Mahera E, Chorti M, Caracciolo V, Sulimenko T, Riga D, Trakas N, Emmanouilidou A, Giordano A, Dráber P, Katsetos CD. Overexpression of γ -tubulin in non-small cell lung cancer. *Histol Histopathol* 2012; **27**: 1183-1194 [PMID: [22806905](https://pubmed.ncbi.nlm.nih.gov/22806905/) DOI: [10.14670/HH-27.1183](https://doi.org/10.14670/HH-27.1183)]
 - 28 **Niu Y**, Liu T, Tse GM, Sun B, Niu R, Li HM, Wang H, Yang Y, Ye X, Wang Y, Yu Q, Zhang F. Increased expression of centrosomal alpha, gamma-tubulin in atypical ductal hyperplasia and carcinoma of the breast. *Cancer Sci* 2009; **100**: 580-587 [PMID: [19215229](https://pubmed.ncbi.nlm.nih.gov/19215229/) DOI: [10.1111/j.1349-7006.2008.01075.x](https://doi.org/10.1111/j.1349-7006.2008.01075.x)]
 - 29 **Caracciolo V**, D'Agostino L, Dráberová E, Sládková V, Crozier-Fitzgerald C, Agamanolis DP, de Chadarevian JP, Legido A, Giordano A, Dráber P, Katsetos CD. Differential expression and cellular distribution of gamma-tubulin and betaIII-tubulin in medulloblastomas and human medulloblastoma cell lines. *J Cell Physiol* 2010; **223**: 519-529 [PMID: [20162618](https://pubmed.ncbi.nlm.nih.gov/20162618/) DOI: [10.1002/jcp.22077](https://doi.org/10.1002/jcp.22077)]
 - 30 **Corvaisier M**, Alvarado-Kristensson M. Non-Canonical Functions of the Gamma-Tubulin Meshwork in the Regulation of the Nuclear Architecture. *Cancers (Basel)* 2020; **12**: 3102 [PMID: [33114224](https://pubmed.ncbi.nlm.nih.gov/33114224/) DOI: [10.3390/cancers12113102](https://doi.org/10.3390/cancers12113102)]
 - 31 **Kállai BM**, Kourová H, Chumová J, Papdi C, Trögelová L, Kofroňová O, Hozák P, Filimonenko V, Mészáros T, Magyar Z, Bögre L, Binarová P. γ -Tubulin interacts with E2F transcription factors to regulate proliferation and endocycling in Arabidopsis. *J Exp Bot* 2020; **71**: 1265-1277 [PMID: [31693141](https://pubmed.ncbi.nlm.nih.gov/31693141/) DOI: [10.1093/jxb/erz498](https://doi.org/10.1093/jxb/erz498)]
 - 32 **Herreros L**, Rodríguez-Fernandez JL, Brown MC, Alonso-Lebrero JL, Cabañas C, Sánchez-Madrid F, Longo N, Turner CE, Sánchez-Mateos P. Paxillin localizes to the lymphocyte microtubule organizing center and associates with the microtubule cytoskeleton. *J Biol Chem* 2000; **275**: 26436-26440 [PMID: [10840040](https://pubmed.ncbi.nlm.nih.gov/10840040/) DOI: [10.1074/jbc.M003970200](https://doi.org/10.1074/jbc.M003970200)]
 - 33 **Wang J**, Chen W, Wei W, Lou J. Oncogene TUBA1C promotes migration and proliferation in hepatocellular carcinoma and predicts a poor prognosis. *Oncotarget* 2017; **8**: 96215-96224 [PMID: [29221200](https://pubmed.ncbi.nlm.nih.gov/29221200/) DOI: [10.18632/oncotarget.21894](https://doi.org/10.18632/oncotarget.21894)]
 - 34 **Loong HH**, Yeo W. Microtubule-targeting agents in oncology and therapeutic potential in hepatocellular carcinoma. *Onco Targets Ther* 2014; **7**: 575-585 [PMID: [24790457](https://pubmed.ncbi.nlm.nih.gov/24790457/) DOI: [10.2147/OTT.S46019](https://doi.org/10.2147/OTT.S46019)]
 - 35 **Bhattacharjya S**, Nath S, Ghose J, Maiti GP, Biswas N, Bandyopadhyay S, Panda CK, Bhattacharyya NP, Roychoudhury S. miR-125b promotes cell death by targeting spindle assembly checkpoint gene MAD1 and modulating mitotic progression. *Cell Death Differ* 2013; **20**: 430-442 [PMID: [23099851](https://pubmed.ncbi.nlm.nih.gov/23099851/) DOI: [10.1038/cdd.2012.135](https://doi.org/10.1038/cdd.2012.135)]
 - 36 **Chen H**, Xu Z. Hypermethylation-Associated Silencing of miR-125a and miR-125b: A Potential Marker in Colorectal Cancer. *Dis Markers* 2015; **2015**: 345080 [PMID: [26693202](https://pubmed.ncbi.nlm.nih.gov/26693202/) DOI: [10.1155/2015/345080](https://doi.org/10.1155/2015/345080)]
 - 37 **Jiang Y**, Luan Y, Chang H, Chen G. The diagnostic and prognostic value of plasma microRNA-125b-5p in patients with multiple myeloma. *Oncol Lett* 2018; **16**: 4001-4007 [PMID: [30128020](https://pubmed.ncbi.nlm.nih.gov/30128020/) DOI: [10.3892/ol.2018.9128](https://doi.org/10.3892/ol.2018.9128)]
 - 38 **Wang H**, Tan G, Dong L, Cheng L, Li K, Wang Z, Luo H. Circulating MiR-125b as a marker predicting chemoresistance in breast cancer. *PLoS One* 2012; **7**: e34210 [PMID: [22523546](https://pubmed.ncbi.nlm.nih.gov/22523546/) DOI: [10.1371/journal.pone.0034210](https://doi.org/10.1371/journal.pone.0034210)]
 - 39 **Song S**, Yang Y, Liu M, Liu B, Yang X, Yu M, Qi H, Ren M, Wang Z, Zou J, Li F, Du X, Zhang H, Luo J. MiR-125b attenuates human hepatocellular carcinoma malignancy through targeting SIRT6. *Am J Cancer Res* 2018; **8**: 993-1007 [PMID: [30034937](https://pubmed.ncbi.nlm.nih.gov/30034937/)]
 - 40 **Hua S**, Quan Y, Zhan M, Liao H, Li Y, Lu L. miR-125b-5p inhibits cell proliferation, migration, and invasion in hepatocellular carcinoma via targeting *TXNRD1*. *Cancer Cell Int* 2019; **19**: 203 [PMID: [31384178](https://pubmed.ncbi.nlm.nih.gov/31384178/) DOI: [10.1186/s12935-019-0919-6](https://doi.org/10.1186/s12935-019-0919-6)]
 - 41 **Spizzo R**, Almeida MI, Colombatti A, Calin GA. Long non-coding RNAs and cancer: a new frontier of translational research? *Oncogene* 2012; **31**: 4577-4587 [PMID: [22266873](https://pubmed.ncbi.nlm.nih.gov/22266873/) DOI: [10.1038/onc.2011.621](https://doi.org/10.1038/onc.2011.621)]
 - 42 **Yuan JH**, Yang F, Wang F, Ma JZ, Guo YJ, Tao QF, Liu F, Pan W, Wang TT, Zhou CC, Wang SB, Wang YZ, Yang Y, Yang N, Zhou WP, Yang GS, Sun SH. A long noncoding RNA activated by TGF- β promotes the invasion-metastasis cascade in hepatocellular carcinoma. *Cancer Cell* 2014; **25**: 666-681 [PMID: [24768205](https://pubmed.ncbi.nlm.nih.gov/24768205/) DOI: [10.1016/j.ccr.2014.03.010](https://doi.org/10.1016/j.ccr.2014.03.010)]
 - 43 **Hung T**, Wang Y, Lin MF, Koegel AK, Kotake Y, Grant GD, Horlings HM, Shah N, Umbricht C, Wang P, Kong B, Langerød A, Borresen-Dale AL, Kim SK, van de Vijver M, Sukumar S, Whitfield ML, Kellis M, Xiong Y, Wong DJ, Chang HY. Extensive and coordinated transcription of noncoding RNAs within cell-cycle promoters. *Nat Genet* 2011; **43**: 621-629 [PMID: [21642992](https://pubmed.ncbi.nlm.nih.gov/21642992/) DOI: [10.1038/ng.811](https://doi.org/10.1038/ng.811)]

- 10.1038/ng.848]
- 44 **Rinn JL**, Chang HY. Genome regulation by long noncoding RNAs. *Annu Rev Biochem* 2012; **81**: 145-166 [PMID: 22663078 DOI: 10.1146/annurev-biochem-051410-092902]
 - 45 **Zong X**, Tripathi V, Prasanth KV. RNA splicing control: yet another gene regulatory role for long nuclear noncoding RNAs. *RNA Biol* 2011; **8**: 968-977 [PMID: 21941126 DOI: 10.4161/rna.8.6.17606]
 - 46 **Gibb EA**, Vucic EA, Enfield KS, Stewart GL, Lonergan KM, Kennett JY, Becker-Santos DD, MacAulay CE, Lam S, Brown CJ, Lam WL. Human cancer long non-coding RNA transcriptomes. *PLoS One* 2011; **6**: e25915 [PMID: 21991387 DOI: 10.1371/journal.pone.0025915]
 - 47 **Ji P**, Diederichs S, Wang W, Böing S, Metzger R, Schneider PM, Tidow N, Brandt B, Buerger H, Bulk E, Thomas M, Berdel WE, Serve H, Müller-Tidow C. MALAT-1, a novel noncoding RNA, and thymosin beta4 predict metastasis and survival in early-stage non-small cell lung cancer. *Oncogene* 2003; **22**: 8031-8041 [PMID: 12970751 DOI: 10.1038/sj.onc.1206928]
 - 48 **Tripathi V**, Ellis JD, Shen Z, Song DY, Pan Q, Watt AT, Freier SM, Bennett CF, Sharma A, Bubulya PA, Blencowe BJ, Prasanth SG, Prasanth KV. The nuclear-retained noncoding RNA MALAT1 regulates alternative splicing by modulating SR splicing factor phosphorylation. *Mol Cell* 2010; **39**: 925-938 [PMID: 20797886 DOI: 10.1016/j.molcel.2010.08.011]
 - 49 **Gutschner T**, Hämmerle M, Eissmann M, Hsu J, Kim Y, Hung G, Revenko A, Arun G, Stentrup M, Gross M, Zörnig M, MacLeod AR, Spector DL, Diederichs S. The noncoding RNA MALAT1 is a critical regulator of the metastasis phenotype of lung cancer cells. *Cancer Res* 2013; **73**: 1180-1189 [PMID: 23243023 DOI: 10.1158/0008-5472.CAN-12-2850]
 - 50 **Yang L**, Lin C, Liu W, Zhang J, Ohgi KA, Grinstein JD, Dorrestein PC, Rosenfeld MG. ncRNA- and Pc2 methylation-dependent gene relocation between nuclear structures mediates gene activation programs. *Cell* 2011; **147**: 773-788 [PMID: 22078878 DOI: 10.1016/j.cell.2011.08.054]
 - 51 **Thorner AR**, Hoadley KA, Parker JS, Winkel S, Millikan RC, Perou CM. In vitro and *in vivo* analysis of B-Myb in basal-like breast cancer. *Oncogene* 2009; **28**: 742-751 [PMID: 19043454 DOI: 10.1038/onc.2008.430]
 - 52 **Guo F**, Li Y, Liu Y, Wang J, Li G. Inhibition of metastasis-associated lung adenocarcinoma transcript 1 in CaSki human cervical cancer cells suppresses cell proliferation and invasion. *Acta Biochim Biophys Sin (Shanghai)* 2010; **42**: 224-229 [PMID: 20213048 DOI: 10.1093/abbs/gmq008]
 - 53 **Lai MC**, Yang Z, Zhou L, Zhu QQ, Xie HY, Zhang F, Wu LM, Chen LM, Zheng SS. Long non-coding RNA MALAT-1 overexpression predicts tumor recurrence of hepatocellular carcinoma after liver transplantation. *Med Oncol* 2012; **29**: 1810-1816 [PMID: 21678027 DOI: 10.1007/s12032-011-0004-z]
 - 54 **Lin R**, Maeda S, Liu C, Karin M, Edgington TS. A large noncoding RNA is a marker for murine hepatocellular carcinomas and a spectrum of human carcinomas. *Oncogene* 2007; **26**: 851-858 [PMID: 16878148 DOI: 10.1038/sj.onc.1209846]
 - 55 **Huang M**, Wang H, Hu X, Cao X. lncRNA MALAT1 binds chromatin remodeling subunit BRG1 to epigenetically promote inflammation-related hepatocellular carcinoma progression. *Oncoimmunology* 2019; **8**: e1518628 [PMID: 30546959 DOI: 10.1080/2162402X.2018.1518628]
 - 56 **Zhao ZB**, Chen F, Bai XF. Long Noncoding RNA MALAT1 Regulates Hepatocellular Carcinoma Growth Under Hypoxia via Sponging MicroRNA-200a. *Yonsei Med J* 2019; **60**: 727-734 [PMID: 31347327 DOI: 10.3349/ymj.2019.60.8.727]
 - 57 **Huang Z**, Huang L, Shen S, Li J, Lu H, Mo W, Dang Y, Luo D, Chen G, Feng Z. Sp1 cooperates with Sp3 to upregulate MALAT1 expression in human hepatocellular carcinoma. *Oncol Rep* 2015; **34**: 2403-2412 [PMID: 26352013 DOI: 10.3892/or.2015.4259]
 - 58 **Bagchi D**, Sen CK, Bagchi M, Atalay M. Anti-angiogenic, antioxidant, and anti-carcinogenic properties of a novel anthocyanin-rich berry extract formula. *Biochemistry (Moscow)* 2004; **69**: 75-80, 1 p preceding 75 [PMID: 14972022 DOI: 10.1023/b:biry.0000016355.19999.93]
 - 59 **Thummayot S**, Tocharus C, Jumnonprakhon P, Suksamrarn A, Tocharus J. Cyanidin attenuates A β_{25-35} -induced neuroinflammation by suppressing NF- κ B activity downstream of TLR4/NOX4 in human neuroblastoma cells. *Acta Pharmacol Sin* 2018; **39**: 1439-1452 [PMID: 29671417 DOI: 10.1038/aps.2017.203]
 - 60 **Rugină D**, Hanganu D, Diaconeasa Z, Tăbăran F, Coman C, Leopold L, Bunea A, Pintea A. Antiproliferative and Apoptotic Potential of Cyanidin-Based Anthocyanins on Melanoma Cells. *Int J Mol Sci* 2017; **18** [PMID: 28468289 DOI: 10.3390/ijms18050949]
 - 61 **Mazewski C**, Kim MS, Gonzalez de Mejia E. Anthocyanins, delphinidin-3-O-glucoside and cyanidin-3-O-glucoside, inhibit immune checkpoints in human colorectal cancer cells *in vitro* and *in silico*. *Sci Rep* 2019; **9**: 11560 [PMID: 31399602 DOI: 10.1038/s41598-019-47903-0]
 - 62 **Aiyer HS**, Warri AM, Woode DR, Hilakivi-Clarke L, Clarke R. Influence of berry polyphenols on receptor signaling and cell-death pathways: implications for breast cancer prevention. *J Agric Food Chem* 2012; **60**: 5693-5708 [PMID: 22300613 DOI: 10.1021/jf204084f]
 - 63 **Hyun JW**, Chung HS. Cyanidin and Malvidin from *Oryza sativa* cv. Heugjinjubyeo mediate cytotoxicity against human monocytic leukemia cells by arrest of G(2)/M phase and induction of apoptosis. *J Agric Food Chem* 2004; **52**: 2213-2217 [PMID: 15080622 DOI: 10.1021/jf030370h]
 - 64 **Tsai TC**, Huang HP, Chang KT, Wang CJ, Chang YC. Anthocyanins from roselle extract arrest cell cycle G2/M phase transition via ATM/Chk pathway in p53-deficient leukemia HL-60 cells. *Environ Toxicol* 2017; **32**: 1290-1304 [PMID: 27444805 DOI: 10.1002/tox.22324]
 - 65 **Bishayee A**, Háznagy-Radnai E, Mbimba T, Sipos P, Morazzoni P, Darvesh AS, Bhatia D, Hohmann

- J. Anthocyanin-rich black currant extract suppresses the growth of human hepatocellular carcinoma cells. *Nat Prod Commun* 2010; **5**: 1613-1618 [PMID: 21121259 DOI: 10.1177/1934578X1000501020]
- 66 **Shin DY**, Ryu CH, Lee WS, Kim DC, Kim SH, Hah YS, Lee SJ, Shin SC, Kang HS, Choi YH. Induction of apoptosis and inhibition of invasion in human hepatoma cells by anthocyanins from meoru. *Ann N Y Acad Sci* 2009; **1171**: 137-148 [PMID: 19723048 DOI: 10.1111/j.1749-6632.2009.04689.x]
- 67 **Salmena L**, Poliseno L, Tay Y, Kats L, Pandolfi PP. A ceRNA hypothesis: the Rosetta Stone of a hidden RNA language? *Cell* 2011; **146**: 353-358 [PMID: 21802130 DOI: 10.1016/j.cell.2011.07.014]



Published by **Baishideng Publishing Group Inc**
7041 Koll Center Parkway, Suite 160, Pleasanton, CA 94566, USA
Telephone: +1-925-3991568
E-mail: bpgoffice@wjgnet.com
Help Desk: <https://www.f6publishing.com/helpdesk>
<https://www.wjgnet.com>

